Nuclear Physics **A509** (1990) 269–286
North-Holland

GAMMA VIBRATION AND WOBBLING MOTION IN ^{182}Os

Masayuki MATSUZAKI

Institute of Physics, University of Tsukuba, Ibaraki 305, Japan

Received 12 May 1989
(Revised 27 July 1989)

Abstract: Properties of a positive-parity side band – yrast odd-spin and yrare even-spin sequences – in ^{182}Os are studied by means of the random-phase approximation based on the rotating shell model with triaxial deformation. Two kinds of interpretations on it – the gamma-vibrational band built on the s-configuration and another rotation-aligned two-quasiparticle band – are examined. Although the former is preferable energetically, we need experimental information on $B(E2)$ values to establish such an interpretation. A gradual character-change of the gamma vibration with negative signature to the wobbling motion through the rotational K-mixing in its wave function is discussed. We show a relation between the wobbling model of Bohr and Mottelson and the present approach based on an analytic study.

1. Introduction

Collective rotational motion changes the nuclear mean field. Properties of quadrupole excitation modes made up from the single-particle motions in the mean field are also influenced by the nuclear rotation as a consequence. The rotational effects on them have two aspects. One is gradual change within each rotational band which appears as the rotational K-mixing in the wave function. The other is abrupt change brought about by the rotational alignment of quasiparticles. The latter may also increase the K-mixing. Both aspects were studied extensively from a microscopic point of view by Shimizu and Matsuyanagi [1-3]). The most interesting problem concerning the rotation–vibration interaction in nuclei is the character-change from the gamma vibration with negative signature to the wobbling mode which has been expected to take place when we look at the high-spin continuation of the gamma-vibrational band as discussed by Mikhailov and Janssen [4,5]). Although the existence of the nuclear wobbling mode has been predicted in macroscopic and microscopic models [6–9]), we do not know in what region in the nuclear chart, spin and deformation it really exists.

Level structures of slightly neutron-deficient osmium isotopes have been studied well using (HI, xn) reactions. Among them, a positive-parity side band (even and odd spin), which was interpreted as the yrare rotation-aligned two-quasiparticle band (s′-band) previously [10,11]), was tentatively reinterpreted as the gamma-vibrational band built on the s-configuration recently [12]). This is the second candidate of the sγ-band. Since ^{182}Os is located adjacent to the very gamma-soft heavier

osmium isotopes, we can expect larger triaxial deformation or more collective gamma vibration than the case of the first candidate, ^{164}Er [ref. [13])] to which theoretical efforts were devoted [1-3]). Very recently an even-spin positive-parity side band in ^{118}Xe was also interpreted tentatively as the sγ-band [14]). In this case, however, more experimental information is necessary before we discuss the character of this band.

We study in this paper properties of the positive-parity side band in ^{182}Os by means of the random-phase approximation based on the rotating shell model with triaxiality described in ref. [2]). In sect. 2, we survey the characteristics of experimental data. Results of the calculation including both the collective and non-collective states are presented in sect. 3. In sect. 4, some properties of the wobbling-like excitation are discussed based on the uniformly-rotating-frame picture paying attention to the K-mixing due to the Coriolis interaction. Concluding remarks are given in sect. 5.

2. Characteristics of experimental data

The gamma-vibrational band built on the g-configuration in ^{182}Os is established well and it shows small signature splitting in the routhian in such a way that the positive-signature (even-spin) sequence lies about 20 keV lower than the negative-signature (odd-spin) one [10-12]) (fig. 1).

On the other hand, the existence and the decay path of the band of interest have partly been known but its structure has not been confirmed yet. The band members decay to the yrast states but the gamma rays connecting this band with the gγ-band have not been observed [10-12]). This decay pattern prevents the authors of refs. [10,11]) from interpreting this band as the sγ-band. In addition, the fact that this side band shows as large alignments as those of the s-band also seems to support the interpretation as each signature part of this band is another rotation-aligned band (s'-band). The latter property is expected also for the sγ-band. Both the even- and odd-spin sequences of the band under consideration cross with the gγ-band at lower rotational frequencies than the g-s crossing. This can take place when the excitation energies of the sγ-band relative to the s-band are lower than those of the gγ-band relative to the g-band.

Another interesting property of this side band is the signature splitting in excitation energy. The signature splitting in such a way that the odd-spin sequence is favoured is consistent with the behavior of the unperturbed two-quasiparticle states if the negative-signature (odd-spin) sequence is the AC ($\bar{B}C$ built on AB) configuration and the positive-signature (even-spin) one is the BC ($\bar{A}C$ built on AB) configuration. Here A, B and C are the familiar notations denoting the aligned quasiparticle states associated with the $\nu i_{13/2}$ shell and $\bar{A}$ and $\bar{B}$ indicate the conjugate states of A and B, respectively.

If the collective interpretation is adopted, the experimental signature splitting is consistent with the results of ref. [3]) and the asymmetric rotor model [15,16]) but contrary

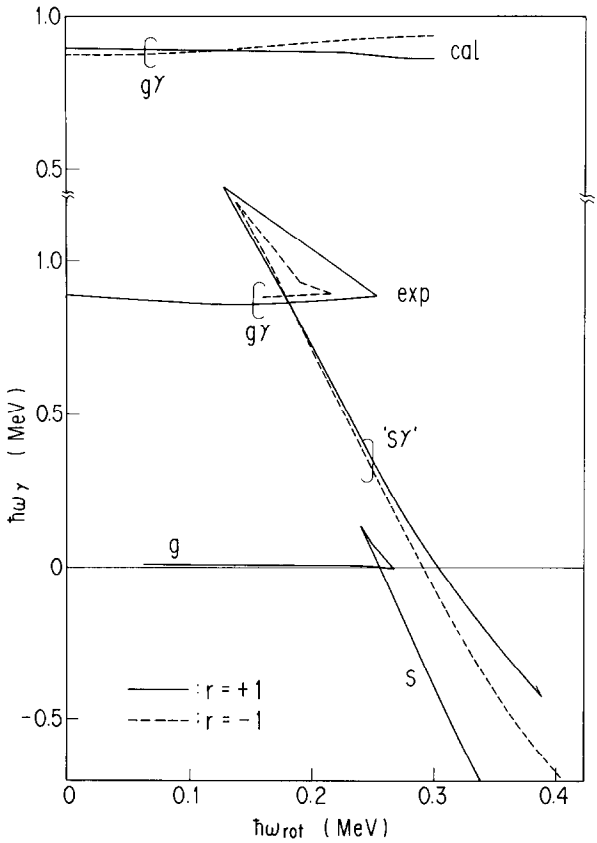

Fig. 1. Calculated excitation energies of the gamma-vibrational band built on the g-configuration as functions of the rotational frequency (upper part). Experimental energy spectra of the yrast and gamma-vibrational bands seen from a reference state ($\mathcal{I}_0 = 23.1\ \hbar^2/\mathrm{MeV}$, $\mathcal{I}_1 = 132.7\ \hbar^4/\mathrm{MeV}^3$)(lower part). Data are taken from ref. [12]) and he positive-parity side band ($r = +1$ and -1) under consideration is denoted by sγ according to this reference but quotation marks are attached since the character of this band has not been established yet. The solid (broken) lines represent the bands with signature $r = +1(-1)$.

to the gamma-unstable model [17]). The magnitude of signature splitting increases as the rotational frequency increases. In addition, the excitation energies measured from the s-band are increasing functions of rotational frequency (fig. 2). The wobbling mode in the model of Bohr and Mottelson in which constant moments of inertia are assumed shows a similar pattern [6]).

3. Microscopic calculation

3.1. DETAILS OF THE CALCULATION

We performed the random-phase-approximation (RPA) calculation in a uniformly-rotating frame in line with refs. [2,3]). The diabatic quasiparticle basis was

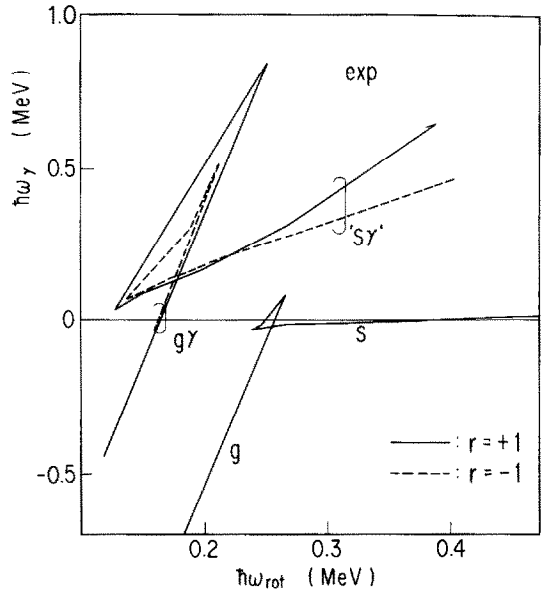

Fig. 2. The same experimental energy spectra as fig. 1 but seen from another reference state [$\mathcal{I}_0 = 32.6\ \hbar^2/\mathrm{MeV}$, $\mathcal{I}_1 = 36.7\ \hbar^4/\mathrm{MeV}^3$, $e_s = 2.35$ MeV and $i_s = 8.31\ \hbar$, see ref. [18])].

constructed making use of the ω_{rot}-expansion up to the second order [19]). Our model contains β- and γ-deformations but the hexadecapole (ε_4) deformation is neglected. Although it is known to be important in this mass region [20]) for the behavior of individual quasiparticle orbitals, we expect to be able to discuss the properties of collective quadrupole excitations quantitatively.

The calculation was performed in the single-particle space consisting of $N_{\mathrm{osc}} = 5$–7 shells for neutrons and $N_{\mathrm{osc}} = 4$–6 shells for protons. We adopted the pairing plus doubly-stretched quadrupole interaction as the residual interaction between quasiparticles. We used the standard coupled dispersion equation for the RPA, eq. (2.25) of ref. [2]), i.e., we did not factorize out the Nambu-Goldstone mode analytically. Referring to the energy-minimization calculation for ^{180}Os [table 4 of ref. [21])], the mean-field parameters and the force strengths were fixed within each reference configuration. These parameters are listed in table 1. The chemical potentials were determined at each rotational frequency so as to give the correct particle numbers.

3.2. RESULTS OF THE CALCULATION

3.2.1. The gγ-band. We chose a standard parameter set for the ground band except for ε_4-deformation; we adopted $\gamma^{(\mathrm{pot})} = -10°$ (in the Lund convention), which was shown to give a good description of the band-crossing frequency when the ε_4-deformation was also included [22]), and then $\beta^{(\mathrm{pot})}$ was determined so as to reproduce the observed $Q_t(2^+ \to 0^+)$ [ref. [23])] using Δ^{oe}'s. The resulting first band-

TABLE 1

Parameters used in the calculation. The sign of γ conforms to the Lund convention. The units are defined as $\hbar\omega_0 = 41A^{-1/3}$ MeV and $b_0^2 = \hbar/M\omega_0$. The upper (lower) numbers in each line are those for the g-band (s-band)

$\beta^{(\mathrm{pot})}$	$\gamma^{(\mathrm{pot})}$	Δ_n (MeV)	Δ_p (MeV)
0.22	−10°	1.05	1.03
0.22	−20°	0.74	0.98

G_n	G_p	$\kappa_0^{(+)}$	$\kappa_1^{(+)}$	$\kappa_2^{(+)}$	$\kappa_1^{(-)}$	$\kappa_2^{(-)}$
1.42	1.71	3.64	3.96	4.15	3.96	4.23
1.42	1.71	3.80	3.96	3.60	3.96	4.23

Units for $G_{n,p}$ are in $10^{-2}\hbar\omega_0$.
Units for $\kappa_K^{(\pm)}$ are in $10^{-3}\hbar\omega_0/b_0^4$.

crossing frequency is 0.308 MeV, which is larger than the experimental value 0.256 MeV because of neglect of ε_4-deformation [20]). The aligned angular momentum at $\hbar\omega_{\mathrm{rot}} = 0.256$ MeV, however, is $8.5\hbar$, which coincides well with the observed value $8.3\hbar$.

The doubly-stretched quadrupole-force strengths for the positive-signature sector were fixed so as to reproduce the beta- and gamma-band-head energies [24]) and to restore the rotational invariance. (As for $\hbar\omega_\beta$, we adopted that of ^{180}W because the beta-vibrational state in ^{182}Os is not known experimentally.) The resulting excitation energy in a rotating frame, $\hbar\omega_{g\gamma(+)}$, is slightly down-sloping with respect to the rotational frequency (fig. 1). Since the RPA dispersion equation decouples to two signature sectors, we can choose different values for $\kappa_1^{(-)}$ and $\kappa_2^{(-)}$ from $\kappa_1^{(+)}$ and $\kappa_2^{(+)}$. Assuming $\kappa_1^{(-)} = \kappa_1^{(+)}$ for simplicity, we adopted a larger value for $\kappa_2^{(-)}$ than $\kappa_2^{(+)}$ in order to reproduce the small signature splitting in the gγ-band. The resulting $\hbar\omega_{g\gamma(-)}$ is slightly up-sloping (fig. 1). This presents a sharp contrast to the calculation based on an axially-symmetric mean field. In the latter case, both $\hbar\omega_{g\gamma(+)}$ and $\hbar\omega_{g\gamma(-)}$ are up-sloping and the signature splitting is reproduced with a signature-independent κ_2. Here we note that this pattern resembles the experimental data on ^{180}Os where γ-deformation is thought to be smaller [21]).

The difference between $\kappa_2^{(+)}$ and $\kappa_2^{(-)}$, which reproduce the experimental signature splitting in the gγ-band, becomes small when $\kappa_0^{(+)}$ is weakened. This fact indicates that the gamma vibration with positive signature is pushed down by the beta vibration lying at a higher energy than the gamma vibrations, since triaxial mean fields bring about the $\Delta K = 2$ mixing between RPA modes already at $\hbar\omega_{\mathrm{rot}} = 0$. Such an effect is absent in the negative-signature sector in accord with the fact that there is no

$K = 0$ mode in it. Consequently κ_2's which reproduce such small signature splitting become signature dependent.

3.2.2. Excitation energies and structures of the RPA modes built on the s-band. The mean field for the s-band is thought to be somewhat more triaxial than that for the g-band in this mass region because of the polarization effect associated with the aligned $(\nu i_{13/2})^2$. The calculation for ^{180}Os by Lieder *et al.* shows that the g–s crossing brings about a change of $\sim 10°$ in γ [ref. [21])]. Referring to it, we adopted $\gamma^{(\mathrm{pot})} = -20°$ and the same $\beta^{(\mathrm{pot})}$ as for the g-band. The pairing gaps for the s-configuration were calculated at $\hbar\omega_{\mathrm{rot}} = 0.2$ MeV using the pairing-force strengths which gave Δ^{oe}'s at the ground state and then these values were fixed.

As mentioned in the previous sections, there are two kinds of interpretations on the observed positive-parity side band. Our RPA calculation gives two normal modes at $\hbar\omega \lesssim 0.9$ MeV in the negative-signature sector when we use the same force strengths $\kappa_1^{(-)}$ and $\kappa_2^{(-)}$ as those for the $g\gamma(-)$-band. One is the gamma-vibration-like collective mode, the other is the $(\nu i_{13/2})^2$-like non-collective mode. The collective solution lies lower in energy and its high-spin part coincides well with the observed states (left-hand part of fig. 3). If we interpret the observed odd-spin sequence as the $s\gamma(-)$-band, there is some deviation between experiment and calculation in the low-spin region. This situation may be related to the fact that the g–s interaction strength is intermediate in ^{182}Os [see fig. 7 of ref. [21]) for example] while we adopted the diabatic basis. The obtained $s\gamma(-)$-solution is very collective and strongly K-mixed. The sum of squared backward amplitudes, which is a measure of collectivity, is presented in fig. 4. The corresponding values for the $g\gamma(\pm)$-bands are 0.79–0.59. Detailed properties of the $s\gamma(-)$-band will be discussed in sect. 4.

The non-collective solution (the perturbed s′-band) also contains the effect of the residual interaction. This solution is mainly composed of the AC ($\bar{B}C$ built on AB)

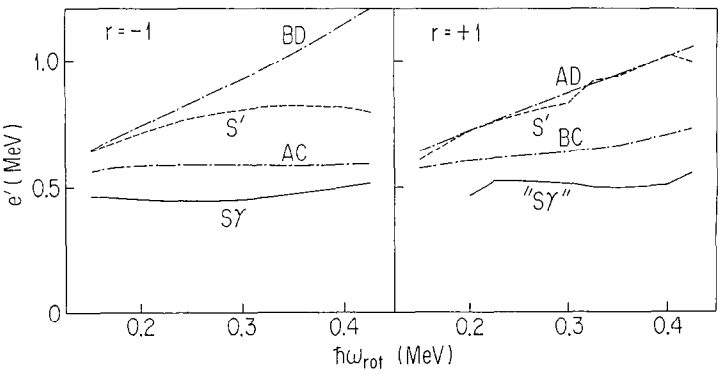

Fig. 3. Lowest two unperturbed $(\nu i_{13/2})^2$ bands and RPA solutions built on the s-band in the negative-signature (left-hand part) and positive-signature (right-hand part) sectors. The solid (broken) lines represent the lowest (second-lowest) RPA solutions. The dot-dashed lines represent unperturbed $(\nu i_{13/2})^2$ bands.

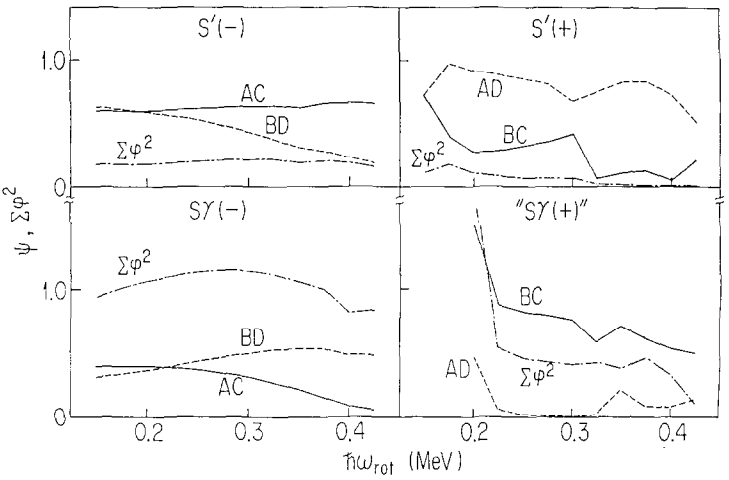

Fig. 4. Forward amplitudes of the lowest two $(\nu i_{13/2})^2$ components in the two RPA solutions in each signature sector (solid and broken lines). Sums of squared backward amplitudes are also shown by dot-dashed lines.

and BD ($\bar{A}D$ built on AB) configurations. The former is $(r=-i)^2$ while the latter is $(r=+i)^2$. Two-quasiproton components are also contained; they produce electric-transition matrix elements which will be discussed in the next subsection. The main components in both the collective and non-collective solutions are shown in the left-hand part of fig. 4.

In order to see the sensitivity of the above results to the used $\kappa_1^{(-)}$ and $\kappa_2^{(-)}$, we examined the force-strengths-free dispersion equation (eq. (4.3)). Aside from some numerical deviation due to the space truncation in the identities used in its derivation (see tables II and III of ref. [2])), it reproduces the results including $B(\mathrm{E2}: \Delta I=1)$'s well (see next subsection).

In the positive-signature sector, we did not obtain any $s\gamma$-like solution when we used the same $\kappa_K^{(+)}$'s as for the $g\gamma(+)$-band. In order to examine whether the $s\gamma(+)$-like solution exists or not, we adjusted the force strengths phenomenologically. Here we note again that this adjustment does not have any influence on the negative-signature sector. We obtained an $s\gamma(+)$-like solution when we weakened $\kappa_2^{(+)}$ and then we tuned $\kappa_2^{(+)}$ and $\kappa_0^{(+)}$ so as to satisfy the following two conditions: (i) $\hbar\omega_{\text{"s}\gamma(+)\text{"}} > \hbar\omega_{s\gamma(-)}$, (ii) the slope of $\hbar\omega_{\text{"s}\gamma(+)\text{"}}$ with respect to $\hbar\omega_{\mathrm{rot}}$ is not largely negative. Here "$s\gamma(+)$" denotes the $s\gamma(+)$-like solution obtained by using adjusted force strengths. We found that such solutions existed on a curve in the $\kappa_2^{(+)}$-$\kappa_0^{(+)}$ plane. The resulting two low-energy normal modes are shown in the right-hand part of fig. 3. There is some irregular behavior in the low-spin region of the lowest solution. Some non-collective modes and the g-band seen from the s-band appear with steep negative and positive slopes, respectively, but they are not shown.

The main forward amplitudes and the sums of squared backward amplitudes associated with both solutions are shown in the right-hand part of fig. 4. The second-lowest solution is mainly composed of the AD ($\bar{B}D$ built on AB) configuration which is the second-lowest unperturbed $(\nu i_{13/2})^2$ state in the positive-signature sector. Therefore this solution is a perturbed s′-band. The main forward strength of the lowest unperturbed $(\nu i_{13/2})^2$ state, the BC ($\bar{A}C$ built on AB) configuration, is contained in the lowest solution which has rather large collectivity. This is a clear difference from the negative-signature sector where the second-lowest RPA solution has the main strength of the lowest unperturbed $(\nu i_{13/2})^2$ configuration. In this sense, the character of the lowest RPA solution in the positive-signature sector obtained by using an adjusted force-strength set is considered to be intermediate between the sγ(+)-band and a perturbed s′-band while the one in the negative-signature sector has a pure collective nature irrespective of $\kappa_1^{(-)}$ and $\kappa_2^{(-)}$.

3.2.3. Electric-transition properties of the RPA modes built on the s-band. Electric-quadrupole-transition rates between RPA modes and the reference band can be calculated making use of Marshalek's formula [25]):

$$B(\mathrm{E2}: I_{\mathrm{RPA}} \to (I-\Delta I)_{\mathrm{ref}}) = |\Lambda^{(\Delta I)}|^2 , \tag{3.1}$$

$$\Lambda^{(\Delta I)} = [Q'_{-\Delta I}, X^{\dagger}]_{\mathrm{RPA}} , \tag{3.2}$$

where $Q'_{-\Delta I}$ ($\Delta I = 0, 1, 2$) are the quadrupole operators quantized along the rotation axis (x-axis) and given as

$$\begin{aligned} Q'_0 &= \sqrt{\tfrac{1}{2}}(-\tfrac{1}{2}Q_0^{(+)} + \sqrt{\tfrac{3}{2}}Q_2^{(+)}) , \\ Q'_{-1} &= i\sqrt{\tfrac{1}{2}}(Q_1^{(-)} - Q_2^{(-)}) , \\ Q'_{-2} &= \sqrt{\tfrac{1}{2}}(-\tfrac{1}{2}\sqrt{3}Q_0^{(+)} + Q_1^{(+)} - \tfrac{1}{2}Q_2^{(+)}) , \end{aligned} \tag{3.3}$$

where

$$Q_K^{(\pm)} = \frac{1}{\sqrt{2(1+\delta_{K0})}}(Q_{+K} \pm Q_{-K}) . \tag{3.4}$$

Henceforth we adopt a notation

$$T_K^{n(\pm)} = [Q_K^{(\pm)}, X_{n(\pm)}^{\dagger}]_{\mathrm{RPA}} \tag{3.5}$$

for the transition amplitudes associated with RPA phonons. Here n (= sγ or s′) specifies the character of each solution and K runs 0, 1, 2 for $r = +1$ and 1, 2 for $r = -1$, respectively. As indicated by the superscripts in the right-hand side of eqs. (3.3), transitions with $\Delta I = 0$ and 2 connect the positive-signature sequence with the s-band while those with $\Delta I = 1$ connect the negative-signature one with the s-band.

Calculated $B(\mathrm{E2}: \Delta I = 1)$ values associated with the transitions from the two sequences in the negative-signature sector to the s-band are shown in the left-hand part of fig. 5. Their ω_{rot}-dependence is completely different from each other. The Coriolis interaction increases the K-mixing in the wave function of both solutions,

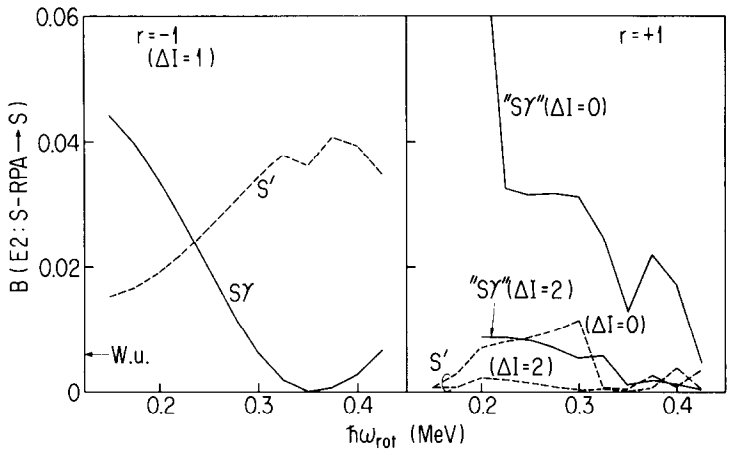

Fig. 5. Calculated B(E2: s-RPA → s) with $\Delta I = 1$ (left-hand part) and with $\Delta I = 0$ and 2 (right-hand part) for the lowest two RPA solutions in each signature sector. The Weisskopf unit for B(E2) is also indicated.

i.e., $|T_2^{n(-)}/T_1^{n(-)}|$ approaches unity, as $\omega_{\rm rot}$ increases. Since $T_1^{s\gamma(-)}$ and $T_2^{s\gamma(-)}$ have the same sign (see sect. 4), B(E2: s$\gamma(-)$ → s) decreases as the K-mixing develops. In contrast, B(E2: s'$(-)$ → s) increases with $\omega_{\rm rot}$ since $T_1^{s'(-)}$ and $T_2^{s'(-)}$ have the opposite sign except for $\hbar\omega_{\rm rot} \lesssim 0.2$ MeV where the former is nearly zero. Therefore we will be able to judge the character of the observed odd-spin sequence by measuring these values.

In the positive-signature sector, there are two kinds of E2 transitions, $\Delta I = 0$ and 2. Since $T_0^{n(+)}$ and $T_2^{n(+)}$ have the opposite sign, B(E2: $\Delta I = 0$) values are larger than B(E2: $\Delta I = 2$) in both solutions. The irregular behavior at the high-spin region is due to the crossings with other non-collective solutions.

The in-band transition probability, which is common to the s-band and excited bands built on it in the present framework, is given by

$$B(\mathrm{E2}: I \to I-2) = \langle Q'_{-2} \rangle^2 . \tag{3.6}$$

The resulting value is about 1.5 $e^2\mathrm{b}^2$ in the whole calculated region, which is enhanced due to the triaxiality $\gamma < 0$.

4. Nuclear wobbling mode as the high-spin continuation of s$\gamma(-)$-band

A possible collective excitation mode in the near-yrast region of rapidly rotating triaxial nuclei was discussed by Bohr and Mottelson [6]). The excitation energy of this mode:

$$\hbar\omega = \hbar\omega_{\rm rot}\sqrt{\frac{(\mathcal{J}_x - \mathcal{J}_y)(\mathcal{J}_x - \mathcal{J}_z)}{\mathcal{J}_y \mathcal{J}_z}}, \tag{4.1}$$

where

$$\mathcal{I}_x > \mathcal{I}_y, \mathcal{I}_z \quad \text{and} \quad \mathcal{I}_y \neq \mathcal{I}_z, \tag{4.2}$$

coincides with the case in a classical asymmetric rotor [26]).

From a microscopic point of view, Mikhailov and Janssen showed that when $\langle Q_2^{(+)} \rangle \neq 0$ the dispersion equation for the coupled RPA in the negative-signature sector could be cast into the form [4]):

$$(\omega^2 - \omega_{\text{rot}}^2) \begin{vmatrix} A(\omega) & C(\omega) \\ B(\omega) & D(\omega) \end{vmatrix} = 0, \tag{4.3}$$

where

$$\begin{aligned} A(\omega) &= \omega \mathcal{I}_y(\omega) - \omega_{\text{rot}} \mathcal{I}_{yz}(\omega), \\ B(\omega) &= \omega_{\text{rot}}(\mathcal{I}_y(\omega) - \mathcal{I}_x) - \omega \mathcal{I}_{yz}(\omega), \\ C(\omega) &= \omega_{\text{rot}}(\mathcal{I}_z(\omega) - \mathcal{I}_x) - \omega \mathcal{I}_{yz}(\omega), \\ D(\omega) &= \omega \mathcal{I}_z(\omega) - \omega_{\text{rot}} \mathcal{I}_{yz}(\omega), \end{aligned} \tag{4.4}$$

with

$$\begin{aligned} \mathcal{I}_x &= \langle J_x \rangle / \hbar\omega_{\text{rot}}, \\ \mathcal{I}_y(\omega) &= \sum_{\mu\nu}{}'' \frac{2E_{\mu\nu}(iJ_y(\mu\nu))^2}{E_{\mu\nu}^2 - (\hbar\omega)^2}, \\ \mathcal{I}_z(\omega) &= \sum_{\mu\nu}{}'' \frac{2E_{\mu\nu}(J_z(\mu\nu))^2}{E_{\mu\nu}^2 - (\hbar\omega)^2}, \\ \mathcal{I}_{yz}(\omega) &= \sum_{\mu\nu}{}'' \frac{2\hbar\omega iJ_y(\mu\nu)J_z(\mu\nu)}{E_{\mu\nu}^2 - (\hbar\omega)^2}. \end{aligned} \tag{4.5}$$

Details of the notation in the above equations conform to that in ref. [2]) except that the matrix elements $iJ_y(\mu\nu)$ (which are real numbers) were denoted by $J_y(\mu\nu)$ in table I of ref. [2]). We note that the energy of the Nambu-Goldstone mode was shifted to zero in refs. [4,5]) (see appendix B of ref. [2])). Mikhailov and Janssen discussed that under a certain condition the terms including $\mathcal{I}_{yz}(\omega)$ could be neglected and thus non-spurious modes would satisfy eq. (4.1). In this case, however, moments of inertia $\mathcal{I}_y$ and $\mathcal{I}_z$ defined in eqs. (4.5) depend on the excitation energy and many normal modes are obtained from a dispersion equation. They anticipated that the gamma-vibrational excitation among them changed its character gradually to the wobbling mode at high spin through the K-mixing due to the Coriolis force. Some effects of the rotational K-mixing were discussed, based on a realistic calculation for ^{164}Er, by Shimizu and Matsuyanagi [2]).

Marshalek showed in a different way that eq. (4.3) with $\omega^2 \neq \omega_{\text{rot}}^2$ could be rewritten as [7])

$$(\hbar\omega)^2 = (\hbar\omega_{\text{rot}})^2 \frac{(\mathcal{I}_x - \mathcal{I}_y^{(\text{eff})}(\omega))(\mathcal{I}_x - \mathcal{I}_z^{(\text{eff})}(\omega))}{\mathcal{I}_y^{(\text{eff})}(\omega)\mathcal{I}_z^{(\text{eff})}(\omega)}, \tag{4.6}$$

where

$$\mathcal{I}_y^{(\mathrm{eff})}(\omega) = \mathcal{I}_y(\omega) + \frac{B(\omega)}{D(\omega)}\,\mathcal{I}_{yz}(\omega)\,,$$

$$\mathcal{I}_z^{(\mathrm{eff})}(\omega) = \mathcal{I}_z(\omega) + \frac{C(\omega)}{A(\omega)}\,\mathcal{I}_{yz}(\omega)\,. \tag{4.7}$$

Namely, the solution of eq. (4.3) can be a microscopic counterpart of the mode discussed by Bohr and Mottelson without the approximation adopted by Mikhailov and Janssen.

There are a few other theoretical works treating the nuclear wobbling mode [8,9]). Among them, Onishi calculated the excitation energy and its spin dependence in the case of ^{166}Er by means of a time-dependent variational method and the Bohr-Sommerfeld quantization rule [9]). But the wobbling mode has not been identified in actual nuclei. There are some theoretical and experimental information [27-31]) about the precession mode built on the high-K isomers whose shapes are thought to be nearly axially symmetric with respect to the rotation axis (either oblate ($\gamma = 60°$) or prolate ($\gamma = -120°$)). Although this mode also appears as a solution of eq. (4.3), the mean field on which it is built is completely different from the case of ^{182}Os ($-60° < \gamma < 0°$) considered in the present paper. In the following, we study in detail the properties of the s$\gamma(-)$-mode presented in the preceding section with an accent on the K-mixing and the resulting character-change to the wobbling motion.

The calculated moments of inertia (eqs. (4.5) and (4.7)) are presented in fig. 6 as functions of the rotational frequency. The ratio of $\{\mathcal{I}_x, \mathcal{I}_y^{(\mathrm{eff})}(\omega), \mathcal{I}_z^{(\mathrm{eff})}(\omega)\}$ at the high-spin region resembles the irrotational moment of inertia for $\gamma_{\mathrm{intr}} = 20°$. This resemblance seems to mean that the side band of interest can be understood also in terms of the asymmetric rotor model with the irrotational moment of inertia, which has been known to give the signature splitting in such a way that the odd-spin members of the $K = 2$ band are favoured. Since $\mathcal{I}_{yz}(\omega)$ is large (and the ordering of $\{\mathcal{I}_x, \mathcal{I}_y(\omega), \mathcal{I}_z(\omega)\}$ is different), the approximation adopted by Mikhailov and Janssen does not hold.

The results for the g$\gamma(-)$-band are shown in fig. 7 for comparison. The quantity $\mathcal{I}_{yz}(\omega)$ itself and thus the differences between $\{\mathcal{I}_y(\omega), \mathcal{I}_z(\omega)\}$ and $\{\mathcal{I}_y^{(\mathrm{eff})}(\omega), \mathcal{I}_z^{(\mathrm{eff})}(\omega)\}$ are small. Accordingly their approximation holds well in this case. The pattern of $\{\mathcal{I}_x, \mathcal{I}_y^{(\mathrm{eff})}(\omega), \mathcal{I}_z^{(\mathrm{eff})}(\omega)\}$ is completely different from that for the s$\gamma(-)$-band but again their ratio resembles the irrotational moment of inertia for small γ_{intr} except for $\hbar\omega_{\mathrm{rot}} \geq 0.25$ MeV where a two-quasiparticle state becomes lower in energy than the g$\gamma(-)$-band. The change in $\mathcal{I}_x$ caused by the alignment of two quasiparticles is well known. The changes in $\{\mathcal{I}_y(\omega), \mathcal{I}_z(\omega), \mathcal{I}_{yz}(\omega)\}$ are also the direct results of the alignment. Namely, in the right-hand side of eqs. (4.5), $iJ_y(\mu\nu)$ and $J_z(\mu\nu)$ involving the aligned orbitals become large in addition to the fact the denominators of these terms become small. As a result $\mathcal{I}(\omega)$'s become large. In

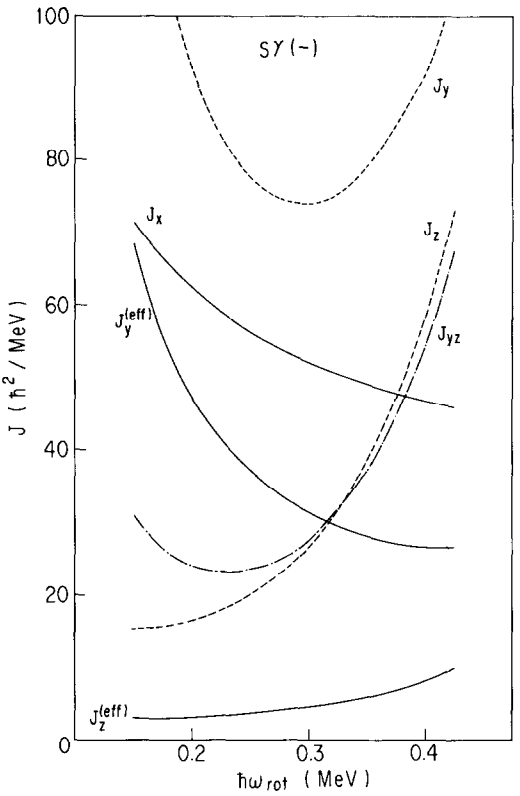

Fig. 6. Calculated dynamical moments of inertia of the sγ(−)-band as functions of the rotational frequency. Their definitions are given in the text.

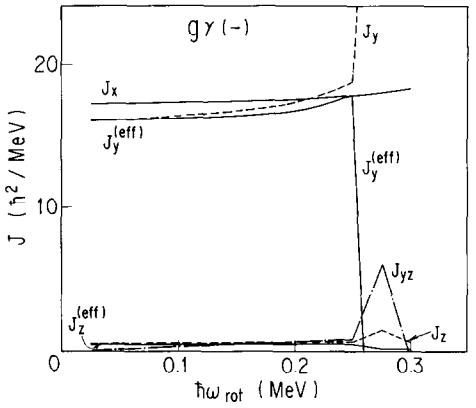

Fig. 7. Same as fig. 6 but for the gγ(−)-band. The anomalous behavior at $\hbar\omega_{rot} > 0.25$ MeV is due to the crossing with a two-quasiparticle band.

^{186}Os, $B(\mathrm{E2}: 0_g \to 2_\gamma)$ in addition to $B(\mathrm{E2}: 0_g \to 2_g)$ is known; [32,33]), the ratio of them gives the zero-point amplitude $\gamma_0 \simeq 17°$. If we assume a similar γ_0 also for ^{182}Os, we can consider that the g-band ($\gamma^{(\mathrm{pot})} = -10°$ adopted) is situated at the vibrational region while the s-band ($\gamma^{(\mathrm{pot})} = -20°$ adopted) is situated at the rotational region with respect to the γ-degree of freedom.

The feature of the rotational K-mixing can be seen directly in the ω_{rot}-dependence of the transition amplitudes associated with the RPA mode under consideration. Their ratio is shown in fig. 8. The isoscalar amplitudes $\tilde{T}_K^{(-)}$ are defined as

$$\tilde{T}_K^{(-)} = [\tilde{Q}_K^{(-)}, X_{s\gamma(-)}^{\dagger}]_{\mathrm{RPA}}, \tag{4.8}$$

where the quantities with tilde denote the doubly-stretched ones [2]). Making use of eqs. (4.3), (4.4) and (4.5), this ratio can be expressed analytically as

$$\frac{\tilde{T}_2^{(-)}}{\tilde{T}_1^{(-)}} = -\frac{2\alpha_2}{\sqrt{3}\alpha_0 - \alpha_2} \frac{\kappa_1^{(-)}}{\kappa_2^{(-)}} \frac{C(\omega)}{D(\omega)}, \tag{4.9}$$

where α_K's are the deformation parameters of a rotating potential

$$h' = h_{\mathrm{sph}} - \sum_{K=0,2} \alpha_K Q_K^{(+)} - \hbar\omega_{\mathrm{rot}} J_x. \tag{4.10}$$

The factor including α_K's in eq. (4.9) can be expressed as a function of $\gamma^{(\mathrm{pot})}$ (appendix B of ref. [34])):

$$\frac{2\alpha_2}{\sqrt{3}\alpha_0 - \alpha_2} = -\frac{\sin\gamma^{(\mathrm{pot})}}{\sin(\gamma^{(\mathrm{pot})} + 60°)}. \tag{4.11}$$

Here we note that the sign of γ is defined oppositely in ref. [34]).

Since we can show that the ratio $C(\omega)/D(\omega)$ associated with the collective mode is negative definite by utilizing the relation between the microscopic and macroscopic models (see eq. (4.21) and the discussion following it), we can discuss the γ-dependence of the relative sign between $\tilde{T}_1^{(-)}$ and $\tilde{T}_2^{(-)}$. This relative sign has never

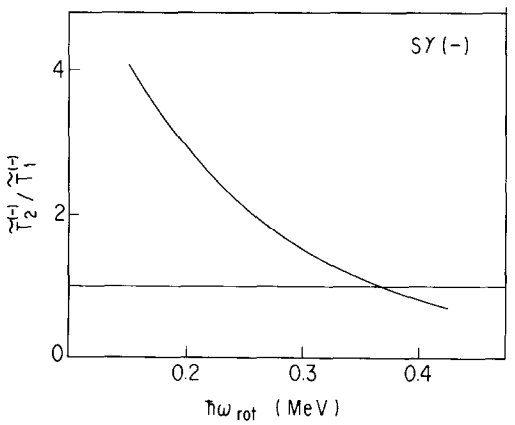

Fig. 8. Ratio of the doubly-stretched isoscalar-quadrupole-transition amplitudes associated with the $s\gamma(-)$-band.

been discussed up to now although it has important physical meanings. As was discussed in sect. 3, the behavior of $B(\mathrm{E2}: s\gamma(-) \to s)$ is a direct result of the coherence between the proton part of the transition amplitudes. Here we note that the ratio of the proton amplitudes and that of the isoscalar amplitudes coincides well because of the isoscalar character of the mode under consideration. The above phase rule, on the other hand, gives an interesting prediction; the ratio $\tilde{T}_2^{(-)}/\tilde{T}_1^{(-)}$ is negative and thus the $B(\mathrm{E2}: \Delta I = 1)$ will increase as the rotational K-mixing develops in the case of the precession mode built on either near-prolate or near-oblate mean fields. This prediction is consistent with the fact that this mode is excited by an operator Q'_{+1} [refs. [27-31])] and thus

$$|\langle -|X_{\mathrm{P}} Q'_{+1}|-\rangle| = |[X_{\mathrm{P}}, Q'_{+1}]_{\mathrm{RPA}}| = \sqrt{\tfrac{1}{2}}|T_1^{(-)} - T_2^{(-)}| \tag{4.12}$$

is large. Since the precession mode built on near-oblate mean fields is the mode to which the gamma vibrations in nuclei with $\gamma > 0$ change their character through the K-mixing, the $B(\mathrm{E2}: \Delta I = 1)$ between the K-mixed collective mode with negative signature and triaxial yrast states will show contrasting behavior depending on the sign of γ.

In addition to the properties of even-even nuclei, this phase rule determines the property of the quasiparticle-vibration-coupling wave function of odd-A nuclei; the K-mixed gamma-vibrational phonon with negative signature mixes strongly into the unfavoured state when $\gamma < 0$ and the first-order vibrational effect is dominant. This is a combined result with the phase rule between the single-particle matrix elements [35]). A numerical example can be found in the "1qp band" case in table I of ref. [19]), where the sign of γ is defined oppositely.

Marshalek discussed a kind of relation between the microscopic and macroscopic descriptions of the nuclear wobbling mode [7]). Eq. (4.9) enables us to present another relation between them. Henceforth we assume the non-stretched quadrupole interaction with a common strength and the Hartree field derived from it for the sake of simplicity. Bohr-Mottelson's wobbling mode is defined, aside from an overall phase, as [6])

$$X_{\mathrm{W}}^{\dagger} = \frac{1}{\sqrt{2\langle J_x \rangle}} \{(x-y) i J_y^{(\mathrm{PA})} - (x+y) J_z^{(\mathrm{PA})}\}, \tag{4.13}$$

where

$$x^2 = \tfrac{1}{2}\left(\frac{\alpha}{\sqrt{\alpha^2 - \beta^2}} + 1\right), \qquad y^2 = \tfrac{1}{2}\left(\frac{\alpha}{\sqrt{\alpha^2 - \beta^2}} - 1\right), \tag{4.14}$$

with

$$\frac{\alpha}{\hbar^2} = \frac{\hbar\omega_{\mathrm{rot}}}{2}\left(\frac{\mathcal{I}_x}{\mathcal{I}_y} + \frac{\mathcal{I}_x}{\mathcal{I}_z} - 2\right),$$
$$\frac{\beta}{\hbar^2} = \frac{\hbar\omega_{\mathrm{rot}}}{2}\left(\frac{\mathcal{I}_x}{\mathcal{I}_y} - \frac{\mathcal{I}_x}{\mathcal{I}_z}\right). \tag{4.15}$$

The principal-axis (PA) frame components of angular momentum in eq. (4.13) can be expressed in terms of the operators in the uniformly-rotating (UR) frame as [7]

$$iJ_y^{(\mathrm{PA})} = iJ_y^{(\mathrm{UR})} - \frac{\kappa}{2\alpha_2}\langle J_x\rangle Q_2^{(-)},$$

$$J_z^{(\mathrm{PA})} = J_z^{(\mathrm{UR})} - \frac{\kappa}{\sqrt{3}\alpha_0 - \alpha_2}\langle J_x\rangle Q_1^{(-)}, \tag{4.16}$$

where κ is the non-stretched quadrupole-interaction strength. Accordingly eq. (4.13) can be written as

$$X_{\mathrm{W}}^{\dagger} = a_y iJ_y^{(\mathrm{UR})} + a_z J_z^{(\mathrm{UR})} + b_y Q_2^{(-)} + b_z Q_1^{(-)}, \tag{4.17}$$

with

$$a_y = \frac{x-y}{\sqrt{2\langle J_x\rangle}},$$

$$a_z = -\frac{x+y}{\sqrt{2\langle J_x\rangle}},$$

$$b_y = -\frac{\kappa}{2\alpha_2}\langle J_x\rangle a_y,$$

$$b_z = -\frac{\kappa}{\sqrt{3}\alpha_0 - \alpha_2}\langle J_x\rangle a_z. \tag{4.18}$$

The transition amplitudes, therefore, are calculated as

$$T_1^{(-)} = [Q_1^{(-)}, X_{\mathrm{W}}^{+}]_{\mathrm{RPA}} = (\sqrt{3}\langle Q_0^{(+)}\rangle - \langle Q_2^{(+)}\rangle)a_y,$$
$$T_2^{(-)} = [Q_2^{(-)}, X_{\mathrm{W}}^{\dagger}]_{\mathrm{RPA}} = -2\langle Q_2^{(+)}\rangle a_z. \tag{4.19}$$

These equations mean that the transition amplitudes have nothing to do with the second terms in eqs. (4.16) which assure the algebra of the PA components. Since the factor including α_K's in eq. (4.9) can be written in terms of the expectation values of quadrupole operators, requiring a kind of selfconsistency between the potential and the density, as

$$\frac{2\alpha_2}{\sqrt{3}\alpha_0 - \alpha_2} = \frac{2\langle Q_2^{(+)}\rangle}{\sqrt{3}\langle Q_0^{(+)}\rangle - \langle Q_2^{(+)}\rangle}, \tag{4.20}$$

finally we obtain a relation between the microscopic quantities $C(\omega)$ and $D(\omega)$ and the macroscopic ones x and y from eqs. (4.9), (4.20) and (4.19)

$$\frac{C(\omega)}{D(\omega)} = \frac{a_z}{a_y} = \frac{y+x}{y-x}. \tag{4.21}$$

Since $X_{\mathrm{W}}^{\dagger}$ is normalized as $x^2 - y^2 = 1$, $C(\omega)/D(\omega)$ is negative definite. Here we note that it does not hold generally for non-collective modes.

Eq. (4.21) can be obtained also from a direct comparison of the expressions for $B(\mathrm{E2}: I \to I-1)$ without the aid of eq. (4.16) as follows. After substituting eq. (4.20), eq. (4.9) can be rewritten by using the quadrupole moments quantized along the x-axis,

$$\frac{T_2^{(-)}}{T_1^{(-)}} = \frac{\sqrt{3}\langle Q_0' \rangle - \sqrt{2}\langle Q_2' \rangle}{\sqrt{3}\langle Q_0' \rangle + \sqrt{2}\langle Q_2' \rangle} \frac{C(\omega)}{D(\omega)}, \tag{4.22}$$

when the non-stretched quadrupole interaction with a common strength is assumed. The reduced transition probability, therefore, takes the form:

$$B(\mathrm{E2}: I \to I-1) \propto \{\sqrt{3}\langle Q_0' \rangle (C(\omega) - D(\omega)) - \sqrt{2}\langle Q_2' \rangle (C(\omega) + D(\omega))\}^2 . \tag{4.23}$$

On the other hand, it is given in the model of Bohr and Mottelson by

$$\frac{1}{\langle J_x \rangle} (\sqrt{3}\langle Q_0' \rangle x - \sqrt{2}\langle Q_2' \rangle y)^2 . \tag{4.24}$$

Consequently we obtain eq. (4.21) again.

5. Concluding remarks

We have studied the properties of the positive-parity side band of ^{182}Os by means of the RPA based on the rotating shell model with triaxial deformation. Having determined the quadrupole-force strengths which reproduced the $\mathrm{g}\gamma(\pm)$-bands, we performed the RPA calculation for excited bands built on the s-band. In the negative-signature sector, the lowest solution is fully collective and the second solution is a perturbed s′-band. The $B(\mathrm{E2}: \Delta I = 1)$ values between these solutions and the s-band show contrasting ω_{rot}-dependence. These results have been confirmed by using the force-strengths-free dispersion equation. Therefore, by measuring them, we will be able to judge the character of the observed odd-spin sequence although the collective interpretation seems to be preferable in view of the excitation energy. On the other hand, the result for the positive-signature sector is sensitive to force strengths; since we did not obtain any $\mathrm{s}\gamma(+)$-like solution when we used the same $\kappa_{\mathrm{K}}^{(+)}$'s as those for the $\mathrm{g}\gamma(+)$-band, we adjusted them phenomenologically. The character of the resulting lowest even-spin sequence is intermediate between the $\mathrm{s}\gamma$-band and a perturbed s′-band.

Detailed properties of the calculated $\mathrm{s}\gamma(-)$-solution have been studied. In particular, the analyses of the dynamical moments of inertia and the K-mixing feature indicate an incipient character-change to the wobbling motion at its high-spin region. This result is consistent with the Janssen–Mikhailov's prediction that such character-change occurs at $I \sim 20\hbar$ in this mass region [5]), which corresponds to $\hbar\omega_{\mathrm{rot}} \sim$ 0.3 MeV.

A relation between the wobbling model of Bohr and Mottelson and the present approach with the uniformly-rotating-frame language has been discussed by starting from an analytic expression for the ratio of the transition amplitudes. The γ-dependence of it has been derived from this study.

The behavior of the dynamical moments of inertia in addition to the signature splitting in excitation energy seems to indicate the possibility that the properties of the side band may be explained also in terms of the asymmetric rotor model with the irrotational moment of inertia. Such a calculation and also more experimental data are desirable.

The author would like to express his thanks to Prof. K. Matsuyanagi for suggesting the problem and for critical discussions and to Dr. Y.R. Shimizu for useful comments and for providing the computer code. This work was started at the Department of Radioisotopes, Japan Atomic Energy Research Institute and supported in part by the Grant-in-Aid for Scientific Research from the Ministry of Education, Science and Culture (No. 01790182). The author is indebted to Fellowships of the Japan Society for the Promotion of Science for Japanese Junior Scientists.

References

1) Y.R. Shimizu and K. Matsuyanagi, Prog. Theor. Phys. **67** (1982) 1641
2) Y.R. Shimizu and K. Matsuyanagi, Prog. Theor. Phys. **70** (1983) 144
3) Y.R. Shimizu and K. Matsuyanagi, Prog. Theor. Phys. **72** (1984) 799
4) I.N. Mikhailov and D. Janssen, Phys. Lett. **B72** (1978) 303
5) D. Janssen and I.N. Mikhailov, Nucl. Phys. **A318** (1979) 390
6) A. Bohr and B.R. Mottelson, Nuclear structure, vol. II (Benjamin, New York, 1975)
7) E.R. Marshalek, Nucl. Phys. **A331** (1979) 429
8) V.G. Zelevinsky, Nucl. Phys. **A344** (1980) 109
9) N. Onishi, Nucl. Phys. **A456** (1986) 279
10) C. Fahlander and G.D. Dracoulis, Nucl. Phys. **A375** (1982) 263
11) R.M. Lieder *et al.*, Nucl. Phys. **A375** (1982) 291
12) P. Chowdhury *et al.*, contribution to Int. Conf. on nuclear shapes (Crete, Greece, 1987)
13) S.W. Yates *et al.*, Phys. Rev. **C21** (1980) 2366
14) C.B. Moon *et al.*, Z. Phys. **A331** (1988) 111
15) A.S. Davydov and G.F. Filippov, Nucl. Phys. **8** (1958) 237
16) H. Toki and A. Faessler, Z. Phys. **A276** (1976) 35
17) L. Wilets and M. Jean, Phys. Rev. **102** (1956) 788
18) S. Frauendorf, in Nuclear physics, ed. C.H. Dasso, R.A. Broglia and A. Winther (North-Holland, Amsterdam, 1982) p. 111
19) M. Matsuzaki, Y.R. Shimizu and K. Matsuyanagi, Prog. Theor. Phys. **79** (1988) 836
20) J.D. Garrett and S. Frauendorf, Phys. Lett. **B108** (1982) 77
21) R.M. Lieder *et al.*, Nucl. Phys. **A476** (1988) 545
22) M. Diebel, Nucl. Phys. **A419** (1984) 221
23) R.B. Firestone, Nucl. Data Sheets **54** (1988) 307
24) M. Sakai, At. Data Nucl. Data Tables **31** (1984) 399
25) E.R. Marshalek, Nucl. Phys. **A275** (1977) 416
26) L.D. Landau and E.M. Lifshitz, Mechanics (Pergamon, London, 1960)
27) H. Kurasawa, Prog. Theor. Phys. **64** (1980) 2055

28) C.G. Andersson *et al.*, Nucl. Phys. **A361** (1981) 147
29) A. Akbarov *et al.*, Sov. J. Nucl. Phys. **33** (1981) 794
30) P. Arve, Y.S. Chen and G.A. Leander, Phys. Scr. **T5** (1983) 157
31) J. Skalski, Nucl. Phys. **A473** (1987) 40; and references therein
32) M.R. Schmorak, Nucl. Data Sheets **13** (1974) 267
33) S. Raman *et al.*, At. Data Nucl. Data Tables **36** (1987) 1
34) Y.R. Shimizu and K. Matsuyanagi, Prog. Theor. Phys. **71** (1984) 960
35) M. Matsuzaki, Nucl. Phys. **A491** (1989) 433